Egypt. J. Chem. **Vol. 66**, No. 9 pp. 307 - 319 (2023)

Egyptian Journal of Chemistry

http://ejchem.journals.ekb.eg/

Electrochemical Reduction Reaction of Potassium Chromate with Orange G and Giemsa Stain Dyes in HCl Solution Using Cyclic Voltammetry and Quantum Chemistry Properties

Marwa S. Sultan*, Mohamed M. Eldefrawy, Esam A. Gomaa

Chemistry Department, Faculty of Science, Mansoura University, Mansoura, Egypt.

Abstract

The cyclic voltammetry of potassium chromate, K_2CrO_4 was studied in 0.1 mol/L HCl at 291.15 and 299.15 K, respectively, using a glassy carbon electrode. The effects of various scan rates were studied in this medium. Cyclic voltammetry was also done for potassium chromate in the presence of Orange G dye at 291.15K and Giemsa stain dye at 299.15K, and further scan rate effects were discussed. The stability constants and Gibbs free energies of complexation resulting from the interaction of chromate ions with dyes were evaluated and found to be complexation reactions. All the Nicholson parameters for potassium chromate are increased by increase of orange G or giemsa Stain dyes concentration indicating the possibility for using this medium as leaching solution. The molecular Gibbs free energies for potassium chromate are increased by increase dyes concentration till it reached -62.846 K.J using 2 $x10^{-3}$ M Orange G dye and -44.951 K.J using $2x10^{-3}$ M Giemsa Stain dye, The stability constants and Gibbs free energy of complexation of potassium chromate with dyes are decreased by decrease of the scan rate till they reached to 3.069 and -17.107 K.J using 2 $x10^{-3}$ M Orange G dye and 5.056 and -28.961 K.J using $2x10^{-3}$ M Giemsa Stain dye for log stability constant and Gibbs free energy of complexation using scan 0.01 V/Sec scan. Molecular docking was also performed for studying the binding modes between Orange G or Giemsa Stain dyes and active sites of the structure of the SARS-CoV-2 N protein (7N0R).

Keywords electron transfer; rate constant; stability constant; Gibbs free energy of complexation; charge transfer coefficient; diffusion coefficient

1. Introduction

The cyclic voltammetry technique is almost used to study the electrochemical properties of the analyte in solutions [1-3]. Cyclic voltammetry is a method to study information about the ions by measuring the current generated versus the applied voltage to the working electrode. Potential is measured between the working electrode and the counter electrode [4].

Potassium chromate is an inorganic substance which is available and commonly used in chemistry. Many studies are aimed to investigate the inhibitive characteristics of potassium chromate on corrosion behaviour as it is so difficult to oxidize [5]. The reduction of potassium chromate was carried out and studied with several substances in different researches [6].

The objective of this work was investigation of the reduction process of potassium chromate in acidic medium cyclic voltammetrically.The potential reduction of Cr(VI) can be determined from the cathodic peak value of cyclic voltammetry.The cathodic peak was a peak which formed during the reduction of the most negative current. The potential range was varied so that the Cr(VI) would be reduced at the electrode surface. The supposed reduction mechanism of chromate involves the following two steps [7]:

$$Cr(VI) + 2e^- \underset{}{\overset{Rapid}{\rightleftharpoons}} Cr(IV) + 1e^- \overset{Slow}{\rightleftharpoons} Cr(III)$$

*Corresponding author e-mail: cute_chemist_09@yahoo.com.; (Marwa S. Sultan).
Received date 2022-10-24; revised date 2022-12-12; accepted date 2022-12-18
DOI: **10.21608/EJCHEM.2022.170666.7120**

The first step is more rapid than the second one since no coordination change is involved, but the second step requires oxygen coordination for changing from tetrahedral to octahedral and is consequently slower than the first step. The ion $Cr(IV)O_4^{-4}$ is a far superior electron donor than $Cr(VI)O_4^{-2}$ [8].

7-Hydroxy-8-(phenylazo)-1,3-naphthalenedisulfonic acid disodium salt (Orange G dye) and7-(dimethylamino)-3H-phenothiazin-3-iminiumchloride (Giemsa Stain dye) [9] (Fig. 1, 2).

Orange G (OG) belongs to the class of azo dyes. It is a type of monoazo and anionic dye which is dissolved in water and stable at all pH values [10]. It is present as a sodium salt in two tautomeric forms in aqueous solution, while organic solvents favour the azo form [11]. It has been used for different applications, such as medication and as a colourant for cosmetics, before it was subsequently abandoned [12]. Nowadays, it is used in the textile and printing industries for dyeing of materials (such as silk and wool), paper, leather products, etc. Furthermore, Orange G is likewise used in histology in different staining formulations and is also essential to pathologists [13]. The colour of Orange G is due to the presence of an azo group, while the auxochromes ($-OH$, $-SO_3$, etc.) enhance the affinity of the dye [14]. The azo bonds are being adsorbed onto the surface of an adsorbent by a covalent bond, that makes it more resistant to harsh conditions [15].

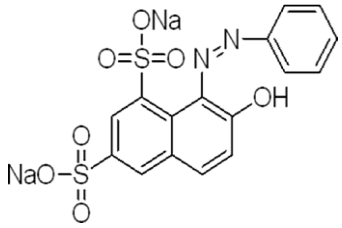

Fig. 1 Structure of Orange G Dye

The stain is usually prepared from commercially available Giemsa powder. Giemsa Stain is specific to the phosphate groups of DNA and attaches itself to where there are big amounts of adenine-thymine bonding.

Giemsa Stain is performed on paraffin sections. It is used to stain the blood cells of hematopoietic tissues. It can also be applied to all tissue sections in which the presence of microorganisms is suspected. This staining does not differentiate gram-positive and gram-negative bacteria [16].

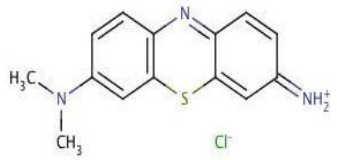

Fig. 2 Structure of Giemsa Stain (GS) dye.

2. Experimental

2.1. Chemicals

The chemicals used like hydrochloric is provided by Sigma Aldrich Company. Potassium chromate is also provided by Sigma Aldrich Company. Orange G and Giemsa Stain dye are produced by Rankem Company.

2.2. Electrolytes

Cyclic voltammetry measurements were performed using 0.1 mol/L HCl. HCl solution was prepared by diluting 37% concentrated acid. The solution of potassium chromate (K_2CrO_4) salt was prepared by appropriate dilution from a 19.479 x 10^{-3}kg in 1 litter (0.1 mol/L). The solution of Orange G dye was prepared by appropriate dissolving 4.524 x 10^{-3} kg in 1 litter (0.01 mol/L) while Giemsa Stain dye was prepared by dissolving 291.8 x 10^{-3} kg in 1 litter (0.01 mol/L). potassium chromate, Orange G and Giemsa Stain dyes were dissolved in de-ionized water.

2.3. Electrodes

The three electrode system was joined to the DY2000 potentiostat. A commercial glassy carbon electrode was used as the working electrode. The platinum wire auxiliary electrode was used and an Ag/AgCl electrode filled with saturated KCl was used as a saturated reference electrode [17-21]. The cell used is a four neck vessel with a capacity of 0.1 L.

2.4. Molecular Docking

The Molecular Operating Environment (MOE) was used as molecular modeling. The molecular modeling and computational calculations were carried out by using DS Biovia material studio 2017, software

material studio 07.0, Gaussian 09 and Docking Server software.

3. Results and Discussion

3.1. Cyclic voltammetry of Cr(VI)

The cyclic voltammograms for different concentrations of Cr(VI)were preceded by 3 x 10^{-2} L of 0.1 mol/L HCl at 291.15K and 299.15K. The resulting data is shown in Fig. 3 and 4 in the range of (1.0V to -1.0V) and (0.7V to -0.1V) starting with 1.0V and -1.0V demonstrating the reduction process. The range of Cr(VI) concentrations used is from 0.332 x 10^{-3} to 6.25 x 10^{-3} mol/L. The reduction wave appears at ~ 0.3 V. We noticed a big reduction wave corresponding to 3 electrons.

The reduction peaks correspond to the following mechanism of reduction:

$$Cr(VI) + 2e^- \underset{}{\overset{\text{Rapid}}{\rightleftharpoons}} Cr(IV) + 1e^- \overset{\text{Slow}}{\rightleftharpoons} Cr(III)$$

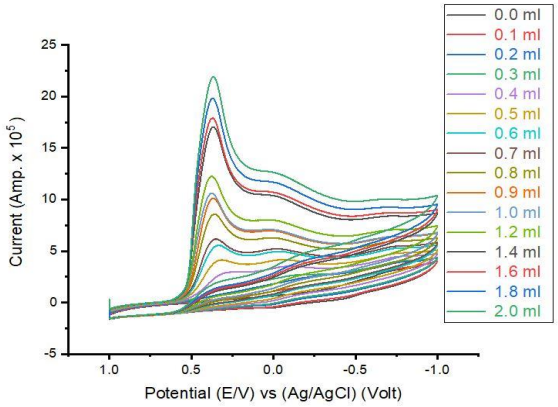

Fig. 3 Cyclic voltammetry of the addition of different amounts of Cr(VI) 0.1 mol/L to 3 x 10^{-2} L HCl 0.1 mol/L, Scan rate 0.1 V. S^{-1}at 291.15K using a glassy carbon electrode.

3.1. Estimation of the cyclic voltammetry data

The different equations [16] applied to the reduction reaction of Cr(VI) are calculated [22-30] such as D_c which is the cathodic diffusion coefficient [31-33]. The heterogeneous electron rate constant from solution to working electrode material was evaluated [34-39].

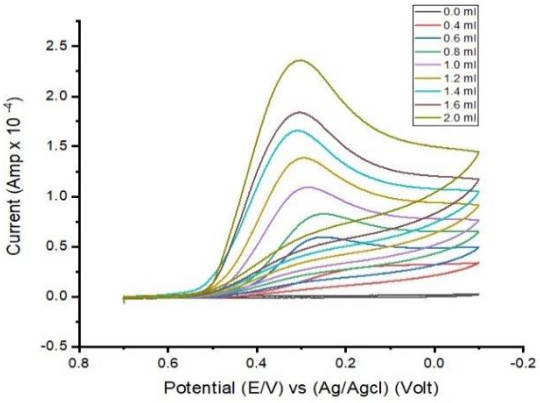

Fig. 4 Cyclic voltammetry of the addition of different amounts of Cr(VI)0.1 mol/L to 3 x 10^{-2} L HCl 0.1 mol/L, Scan rate 0.1 V. S^{-1}at 299.15K using a glassy carbon electrode.

The above parameters can be evaluated for the reduction peak at ~ 0.3 V. [30,45], and the resultant values are presented in (Table 1 - 2).

We noticed the following from (Table 1 - 2):

1 – ΔE_P is a small amount in the range of reversible processes.

2 – i_{pc} values are increased by an increase in Cr (VI) concentrations.

3 – Increasing Cr (VI) concentrations significantly increases the catholic D_c diffusion coefficients, indicating a reversible reaction.

4 – Cathodic surface coverage Γ_c values are increased by an increase in the concentration of Cr (VI) favouring more diffusion.

5 – The cathodic quantity of electricity Q_c and values are largely increased by the increase in the chromium ion concentrations, supporting the diffusion mechanism of the reaction.

3.2. Effect of scan rate on Cr(VI)

The effect of scan rate on Cr (VI) [6.250 x 10^{-3}mol/L] was investigated in both HCl media, and the data found in (Table 3, 4) shows that a decrease in scan rate resulted in an increase in the different solvation parameters, indicating a diffusion-controlled reaction. (Fig. 5, 6) also shows the effect of scan rate on the reduction reaction of the final concentration used of Cr(VI) at 291.15K and 299.15K.

Table 1

shows the thermodynamic and kinetic properties of Cr(VI) at 291.15K and 0.1 $V.s^{-1}$ scan rate in HCl medium.

[M] $x10^3$ $mol.L^{-1}$	$E_{p,c}$ Volt	$I_{p,c}$ $x10^5$ Amp	α_{nac}	D_c $x10^7$ $cm^2.s^{-1}$	$\Gamma_c x10^{10}$ $mol.cm^{-2}$	(+) Q_c $x10^6$ C
0.332	0.386	0.123	1.370	0.0324	0.073	0.412
0.662	0.386	0.335	0.997	0.083	0.197	1.121
0.990	0.386	0.636	0.953	0.138	0.373	2.119
1.316	0.386	1.580	0.891	0.522	0.930	5.285
1.639	0.386	2.936	0.808	1.279	1.727	9.820
1.961	0.386	4.424	0.723	2.268	2.603	14.797
2.280	0.386	5.293	0.696	2.495	3.114	17.707
2.597	0.386	7.699	0.649	4.362	4.529	25.753
2.913	0.386	9.157	0.628	5.066	5.387	30.631
3.226	0.386	9.867	0.556	5.419	5.805	33.006
3.846	0.386	11.448	0.550	5.187	6.735	38.293
4.459	0.386	16.027	0.541	7.695	9.429	53.610
5.063	0.386	16.820	0.525	6.770	9.896	56.265
5.660	0.386	18.890	0.521	6.891	11.114	63.190
6.250	0.386	20.519	0.515	6.744	12.072	68.636

Table 2

shows the thermodynamic and kinetic properties of Cr(VI) at 299.15K and 0.1$V.s^{-1}$scan rate in HCl medium.

[M] $x10^3$ $mol.L^{-1}$	E_{pc} Volt	I_{pc} $x10^5$ Amp	$E_{pc}/2$	α_{nac}	D_c $x10^7$ $cm^2.s^{-1}$	$\Gamma_c x10^{10}$ $mol.cm^{-2}$	(+) Q_c $x10^5$ C
1.316	0.184	0.106	0.241	0.836	0.248	0.638	0.363
1.961	0.258	0.363	0.331	0.664	1.664	2.195	1.248
2.597	0.260	0.509	0.333	0.657	1.887	3.080	1.751
3.226	0.297	0.703	0.370	0.653	2.342	4.250	2.417
3.846	0.303	0.906	0.380	0.622	2.877	5.479	3.115
4.459	0.308	1.084	0.398	0.529	3.598	6.551	3.725
5.063	0.310	1.259	0.402	0.518	3.844	7.613	4.329
6.250	0.311	1.712	0.404	0.516	4.680	10.347	5.883

Table 3 Cyclic voltammetry of Cr(VI) [6.250 $x10^{-3}$mol/L] at different scan at 291.15K in HCl media

ν $V.s^{-1}$	$E_{p,c}$ Volt	$I_{p,c}x10^5$ Amp	α_{nac}	D_c $x10^7$ $cm^2.s^{-1}$	Γ_c $x10^9$ $mol.cm^{-2}$	(+) $Q_c x10^4$ C
0.100	0.386	20.519	0.515	6.744	1.207	0.686
0.050	0.422	12.971	0.617	4.500	1.526	0.868
0.020	0.465	7.970	1.006	2.603	2.344	1.333
0.010	0.483	5.978	1.234	2.388	3.517	2.000

Table 4 Cyclic voltammetry of Cr(VI) [6.250 $x10^{-3}$mol/L] at different scan at 299.15K in HCl media

ν $V.s^{-1}$	E_{pc}Volt	I_{pc} $x10^4$ Amp	α_{nac}	D_c $x10^7$ $cm^2.s^{-1}$	Γ_c $x10^9$ $mol.cm^{-2}$	(+) Q_c $x10^5$ C
0.100	0.311	1.711	0.516	4.680	1.035	5.883
0.050	0.341	1.144	0.661	3.261	1.383	7.862
0.020	0.406	0.699	0.908	2.219	2.113	12.015
0.010	0.457	0.560	1.447	1.789	3.388	19.262

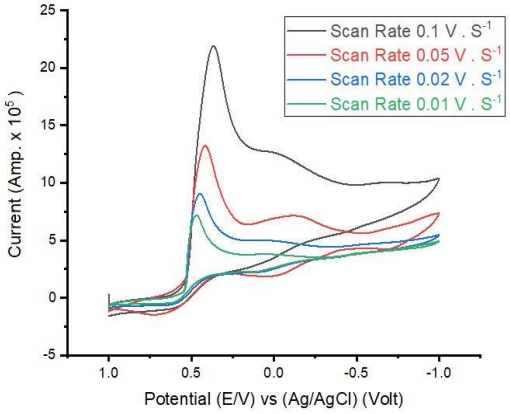

Fig. 5 Cyclic voltammetry of 2 x 10^{-3} L of Cr(VI) 0.1 mol/L + 3 x10^{-2} L HCl 0.1 mol/L at different scan rates at 291.15 K, using a glassy carbon electrode.

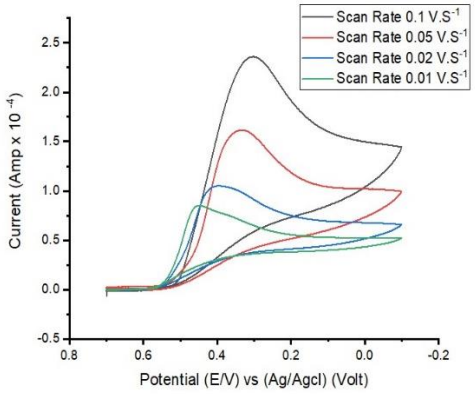

Fig. 6 Cyclic voltammetry of 2 x 10^{-3} L of Cr(VI) 0.1 mol/L + 3 x10^{-2} L HCl 0.1 mol/L at different scan rates at 299.15 K, using a glassy carbon electrode.

3.3. Effect of adding of Orange G or Giemsa Stain dye

Different concentrations of Orange G or Giemsa dye were added to 6.250 x 10^{-3}mol/LCr(VI), within the (1.0 V to -1.0 V) and (0.7V to -0.1V) potential range in HCL medium at 291.15K and 299.15K respectively as shown in (Fig. 7, 8), and the results are shown in (Table 5, 6).

3.4. Effect of adding Orange G or Giemsa dye on ipc for Cr(VI)

In the presence of HCl media, the linear fit of i_{pc} for Cr(VI) in case of adding Orange G dye was drowned, and we prove from them that the increase in reduction current for the Cr(VI) wave by increasing the dye concentration followed by a decrease in reduction current by increasing the amount added from dye, which is due to the complexation behaviour between Cr(VI) and the Orange G dye. (Fig. 9).

While in case of Addition of Giemsa stain dye, we find a decrease of reduction current for the Cr(VI) wave by increasing the Orange G concentration due to the complexation behavior between Cr(VI) and the Orange G dye. (Fig. 10).

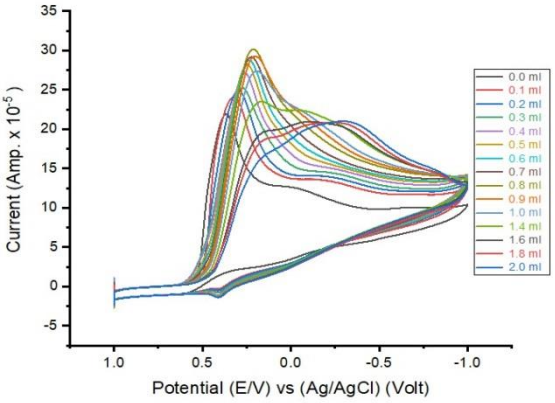

Fig. 7 Cyclic voltammetry of 2 x 10^{-3} L Cr(VI) 0.1 mol/L + 3 x 10^{-2} L HCl 0.1 mol/L in presence of different amounts of Orange G dye 0.01 mol/L, Scan rate 0.1 V. s^{-1}at 291.15 K using a glassy carbon electrode.

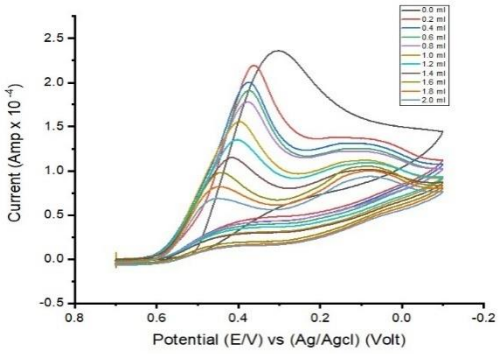

Fig. 8 Cyclic voltammetry of 2 x 10^{-3} L Cr(VI) 0.1 mol/L + 3 x 10^{-2} L HCl 0.1 mol/L in presence of different amounts of Giemsa dye 0.01 mol/L, Scan rate 0.1 V. s^{-1}at 299.15 K using a glassy carbon electrode.

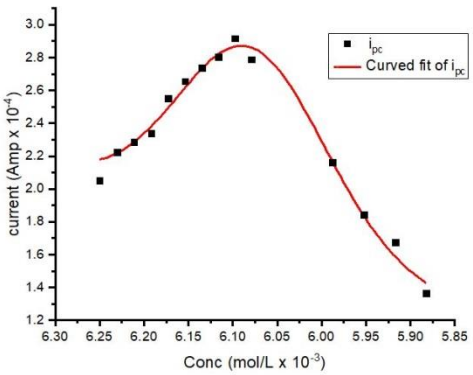

Fig. 9 Change of $i_{pc}$of Cr(VI) by increasing concentration of Orange G dye in HCl media.

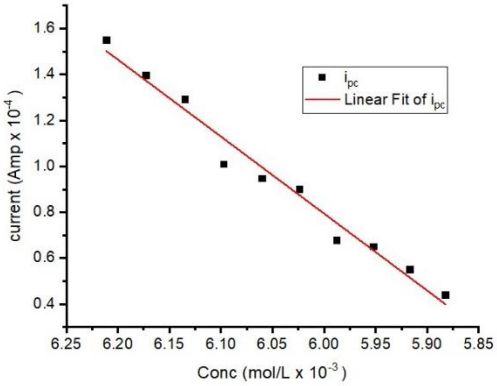

Fig. 10 Change of $i_{pc}$of Cr(VI)by increasing concentration of Giemsa stain dye in HCl media.

We also noticed the following remarks from (Table 5, 6):

1 - The E_{pc} shift favoursCr(VI)-Orange G dye and Cr(VI)-Giemsa Stain dye interaction.

2 - $\Delta E_P$is decreased by an increase in Orange G dye or Giemsa stain dye concentration, favouring complex reactions.

3 - i_{pc}increaseed by increasing the dye concentration, followed by a decrease in its value by increasing the amount of orange G dye added,while in case of addition of Giemsa Stain dye i_{pc} decreased in their values, compared to the absence of the dye, favouring interaction between the metal ions and the dye.

4 - D_c increased by increasing the dye concentration, followed by a decrease in its value by increasing the amount of Orange G dye.WhileD_c decreases in their values, compared to the absence of the Giemsa Stain dye, favouring complex reactions.

5 - α_{na}decreased by increase of Orange G or Giemsa Stain dye concentration due to the attraction of dye with Cr(VI).

6 - Γ_c increased by increasing the dye concentration, followed by a decrease in its value by increasing the amount of Orange G dye,whileΓ_c decreased in their values, compared to the absence of the Giemsa Stain dye, favouring interaction between the metal ions and the dyes.

7 - Increased of Q_c followed by a decrease in its values for Cr(VI)by increase the amount of Orange G dye, while increased of Q_c values for Cr(VI) by adding Giemsa Stain dye than Cr(VI) alone.

3.5. Effect of different scan rates on Cr(VI) with Orange G or Giemsa Stain dye complex

The effects of different scan rates on the interaction of Cr(VI) with Orange G or Giemsa Stain dye were investigated, and the results are shown in (Fig. 11, 12). Most of the data is given in (Table 7, 8). It was noticed that the values increased with the decrease in scan rate, such as Γ_c and Q_c.

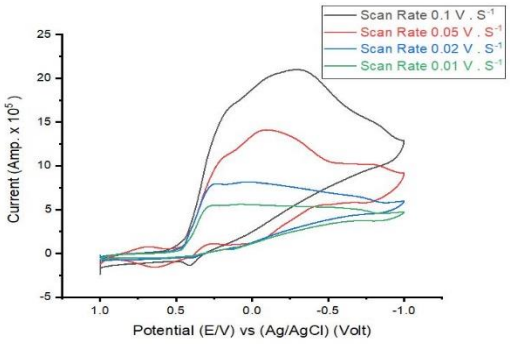

Fig. 11 Cyclic voltammetry of 2 x 10^{-3} L Orange G dye 0.01 mol/L + 2 x 10^{-3} L Cr(VI) 0.1 mol/L + 3 x 10^{-2} L HCl 0.1 mol/L at 291.15K using a glassy carbon electrode at different scan rates.

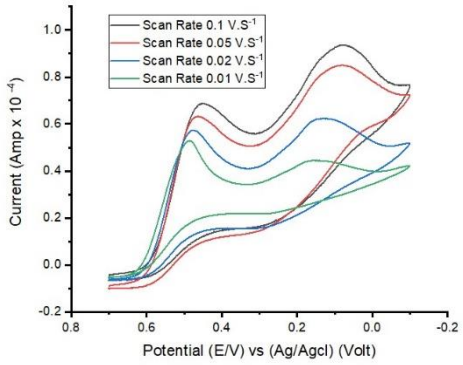

Fig. 12 Cyclic voltammetry of 2 x 10^{-3} L Giemsa Stain dye 0.01 mol/L + 2 x 10^{-3} L Cr(VI) 0.1 mol/L + 3 x 10^{-2} L HCl 0.1 mol/L at 299.15K using a glassy carbon electrode at different scan rates.

On drawing the relation between peak currents i_{pc} and the square root of scan rate ($\upsilon^{1/2}$), straight lines were obtained as shown in (Fig. 13, 14) at 291.15K and (Fig. 15, 16) at 299.15K. The slopes of the line indicate the diffusion reaction mechanism in the presence and absence of dyes.

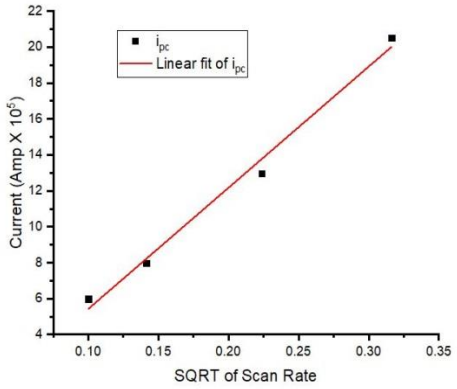

Fig. 13 Relation (i_{pc} Vs. $\nu^{1/2}$) for Cr(VI)at final addition in different scan rates at 291.15K.

Table 5
Kinetic and solvation parameters of Cr(VI) in presence of Orange G dye at 291.15 K and 0.1 scan rate in HCl media

[L] x10^4 mol.L^{-1}	[M] x10^3 mol.L^{-1}	$E_{p,c}$ Volt	$I_{p,c}$ x10^5 Amp	α_{nac}	D_c x10^7 $cm^2.s^{-1}$	Γ_cx10^{10} mol.cm^{-2}	(+) Q_c x10^6 C
0.000	6.250	0.386	20.519	0.515	6.744	12.072	6.864
0.312	6.250	0.348	22.251	0.463	8.876	13.091	7.443
0.621	6.250	0.323	22.847	0.434	10.040	13.441	7.642
0.929	6.250	0.301	23.392	0.424	10.849	13.762	7.825
1.235	6.250	0.285	25.510	0.405	13.579	15.008	8.533
1.538	6.250	0.266	26.553	0.386	15.517	15.622	8.882
1.840	6.250	0.246	27.380	0.362	17.733	16.108	9.159
2.140	6.250	0.232	28.044	0.347	19.528	16.499	9.381
2.439	6.250	0.227	29.172	0.347	21.239	17.162	9.758
2.736	6.250	0.220	27.894	0.347	19.530	16.411	9.331
3.030	6.250	0.207	25.319	0.338	16.614	14.896	8.469
4.192	6.250	0.183	21.615	0.306	13.730	12.716	7.230
4.762	6.250	0.172	18.419	0.296	10.430	10.836	6.161
5.325	6.250	0.165	16.743	0.300	8.585	9.850	5.601
5.882	6.250	0.157	13.660	0.303	5.736	8.036	4.569

Table 6
Kinetic and solvation parameters of Cr(VI) in presence of Giemsa Stain dye at 299.15 K and 0.1 scan rate in HCl media

[M] x10^3 mol.L^{-1}	E_{pc} Volt	i_{pc} x10^4 Amp	$E_{pc}/2$	α_{nac}	D_c x10^7 $cm^2.s^{-1}$	Γ_cx10^{10} mol.cm^{-2}	(+) Q_c x10^5 C
6.211	0.367	1.550	0.424	0.834	2.406	9.371	5.328
6.173	0.380	1.398	0.445	0.743	2.223	8.452	4.806
6.135	0.382	1.292	0.447	0.733	1.947	7.808	4.439
6.098	0.383	1.011	0.449	0.723	1.224	6.109	3.473
6.061	0.402	0.948	0.469	0.711	1.109	5.732	3.259
6.024	0.410	0.900	0.4780	0.706	1.019	5.443	3.095
5.988	0.419	0.679	0.488	0.701	0.590	4.104	2.333
5.952	0.444	0.651	0.514	0.691	0.558	3.937	2.238
5.917	0.453	0.552	0.524	0.681	0.411	3.334	1.896
5.882	0.460	0.440	0.531	0.673	0.268	2.661	1.513

Table 7
Effect of different scan rates on Cr(VI) with Orange G dye complex at 291.15K in HCl media

ν $V.S^{-1}$	$E_{p,c}$ Volt	$I_{p,c}$ x10^5 Amp	D_c x10^7 $cm^2.s^{-1}$	α_{nac}	Γ_c x10^{10} mol.cm^{-2}	(+) Q_c x10^5 C
0.100	0.157	13.660	57.357	0.303	8.036	4.569
0.050	0.222	9.338	40.653	0.399	10.987	6.247
0.020	0.268	6.345	36.337	0.516	18.666	10.613
0.010	0.304	4.386	25.519	0.702	25.805	14.672

Table 8
Effect of different scan rates on Cr(VI) with Giemsa Stain dye complex at 299.15K in HCl media

ν $V.S^{-1}$	$E_{p,c}$ Volt	$I_{p,c}$ x10^5 Amp	D_c x10^7 $cm^2.s^{-1}$	α_{nac}	Γ_c x10^9 mol.cm^{-2}	(+) Q_c x10^4 C
0.100	0.460	4.401	0.268	0.673	0.267	0.151
0.050	0.473	3.828	0.424	0.644	0.463	0.263
0.020	0.486	3.313	0.813	0.628	1.001	0.569
0.010	0.493	3.080	1.414	0.624	1.862	1.059

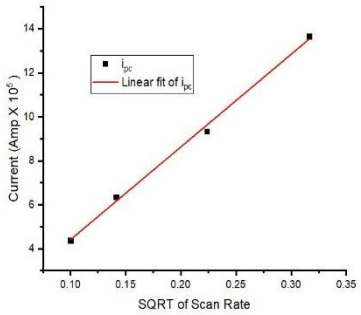

Fig. 14 Relation (i_{pc} Vs. $\nu^{1/2}$) for Cr(VI)at final addition of Orange G dye at 291.15K.

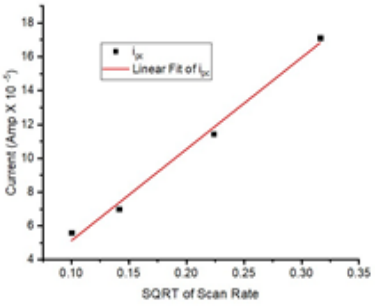

Fig. 15 Relation (i_{pc} Vs. $\nu^{1/2}$) for Cr(VI)at final addition in different scan rates at 299.15K.

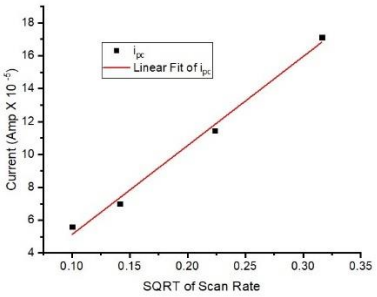

Fig. 16 Relation (i_{pc} Vs. $\nu^{1/2}$) for Cr(VI)at final addition of Giemsa Stain dye at different scan rates at 299.15K

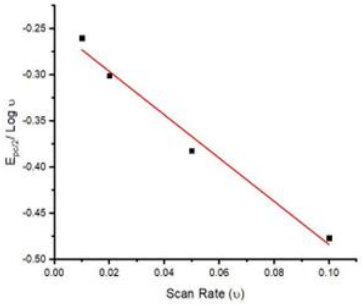

Fig. 17 Relation ($E_{pc/2}$/log υ Vs υ) for Cr(VI)at final addition at 291.15 K.

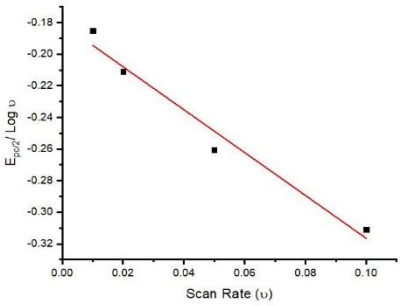

Fig. 18 Relation ($E_{pc/2}$/log υ Vs υ) for Cr(VI)at final addition of Orange G dye at 291.15 K.

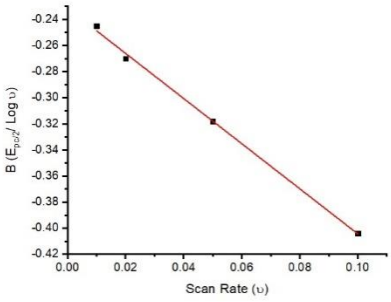

Fig. 19 Relation ($E_{pc/2}$/log υ Vs υ) for Cr(VI)at final addition at 299.15 K.

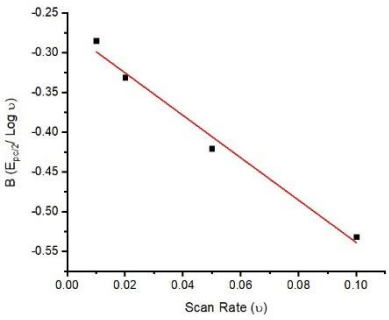

Fig. 20 Relation ($E_{pc/2}$/log υ Vs υ) for Cr(VI)at final addition of Giemsa Stain dye at 299.15 K.

3.6. Thermodynamic parameters for interaction of Cr(VI) with Orange G or Giemsa Stain dye

We used the Langne equation as explained in previous work [24, 30] to calculate the stability constant and Gibbs free energies of complexation for the interaction between Cr(VI) and Orange G and Giemsa Stain G dyes. The evaluated data was given in (Table 9, 10) with the effect of the scan rate data shown also in (Table 11, 12). Very large thermodynamic stability constants β and Gibbs free energy ΔG of complexation

Table 9
Stability constant for Cr(VI) in presence of Orange G dye at 291.15 K and scan rate 0. 1V.s^{-1} in HCl medium

[L] x10^4 mol.L^{-1}	ΔE volt	j	Log[L]	log βj	-ΔG (J/mol)	-ΔG (KJ/mol)
0.312	-0.038	0.005	-7.507	1.940	10816.833	10.817
0.621	-0.063	0.010	-7.207	3.181	17735.390	17.735
0.929	-0.085	0.015	-7.032	4.312	24037.190	24.037
1.235	-0.101	0.020	-6.908	5.093	28391.453	28.391
1.538	-0.120	0.025	-6.813	6.078	33882.490	33.882
1.840	-0.141	0.030	-6.735	7.098	39569.120	39.569
2.141	-0.154	0.035	-6.669	7.776	43349.227	43.349
2.439	-0.159	0.040	-6.613	8.006	44628.794	44.629
2.736	-0.167	0.045	-6.563	8.351	46556.510	46.557
3.030	-0.179	0.050	-6.519	8.972	50016.531	50.017
4.192	-0.203	0.070	-6.378	10.099	56301.531	56.302
4.762	-0.214	0.080	-6.322	10.609	59142.850	59.143
5.325	-0.221	0.090	-6.274	10.913	60836.828	60.837
5.882	-0.229	0.100	-6.230	11.273	62845.671	62.846

Table 10
Stability constant for Cr(VI) in presence of Giemsa Stain dye at 299.15 K and scan rate 0. 1V.s^{-1} in HCl medium

[L] x10^4 mol.L^{-1}	ΔE v	j	Log [L]	Log βj	ΔG (J/mol)	ΔG (KJ/mol)
0.621	0.056	0.010	-4.207	2.884	-16521.845	-16.522
1.235	0.069	0.020	-3.908	3.639	-20845.355	-20.845
1.840	0.070	0.030	-3.735	3.763	-21555.445	-21.555
2.439	0.072	0.040	-3.613	3.899	-22335.498	-22.335
3.030	0.090	0.050	-3.519	4.896	-28043.235	-28.043
3.614	0.099	0.060	-3.442	5.391	-30880.787	-30.881
4.192	0.108	0.07	-3.378	5.921	-33914.218	-33.914
4.762	0.133	0.08	-3.322	7.232	-41422.134	-41.422
5.325	0.142	0.09	-3.274	7.756	-44423.955	-44.424
5.882	0.149	0.1	-3.230	8.148	-46669.268	-46.669

Table 11
Stability constant for different scan rates for Cr(VI) with Orange G dye complex at 291.15 K in HCl media

υ	ΔE mv	Log[L]	Log βj	-ΔG (J/mol)	-ΔG (KJ/mol)
0.100	-0.229	-6.230	-11.273	62845.671	62.846
0.050	-0.214	-6.230	-10.506	58568.696	58.569
0.020	-0.197	-6.230	-9.591	53467.880	53.468
0.010	-0.179	-6.230	-8.676	48366.321	48.366

Table 12
Stability constant for different scan rates for Cr(VI) with Giemsa Stain dye complex at 299.15 K in HCl medium

υ	ΔE mv	Log[L]	Log βj	ΔG (J/mol)	ΔG (KJ/mol)
0.100	0.149	-3.230	8.148	-46669.268	-46.669
0.050	0.131	-3.230	7.260	-41584.889	-41.585
0.020	0.080	-3.230	4.656	-26667.121	-26.667
0.010	0.036	-3.230	2.449	-14025.911	-14.026

[25-45] were obtained, indicating a very strong complexation interaction is happening for the interaction between Cr(VI) and Orange G Giemsa Stain G dyes, forming very strong covalent bonds.

3.7. Molecular docking

SARS-CoV-2 (or 2019-nCoV) belongs to lineage B of the β-coronavirus genus [46]. Coronaviruses are relatively large enveloped, positive-sense, single-stranded RNA (~30 kb) viruses. The SARS-CoV-2 genome encodes four structural proteins and other accessory or non-structural proteins (including the viral pp1a-pp1ab replicase, the 3C-like protease (3CLpro), the papain-like protease (PLpro), and the RNA-dependent RNA-polymerase (RdRp) [47, 48].

A molecular modeling study using the Molecular Operating Environment (MOE) was performed for studying the binding modes between Orange G or Giemsa Stain dyes and active sites of the structure of the SARS-CoV-2 N protein (7N0R), the active antigen for covid-19 virus (Fig. 21-24). The orange G dye interaction report data is shown in (Fig. 25), which is copied from the calculation showing interactions through H-acceptor, ionic and pi-H between the protein and orange G dye. While the report data of Giemsa stain dye appeared in (Fig. 26), the interaction happened through H-acceptor, pi-H and pi-pi.

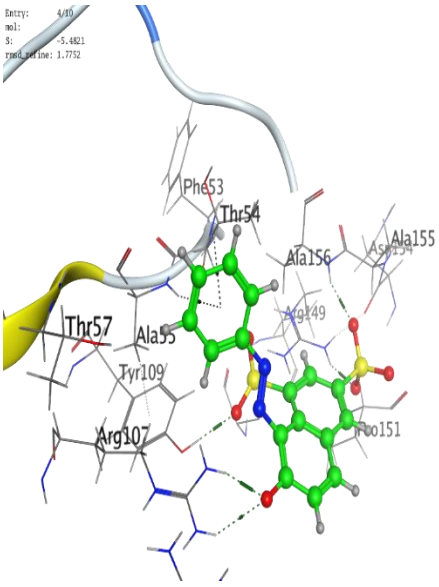

Fig. 21 3D of the binding mode of Orange G with (7N0R) receptor.

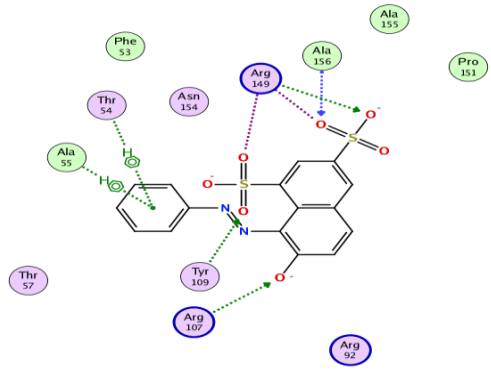

Fig. 22 2D of the binding mode of Orange G with (7N0R) receptor.

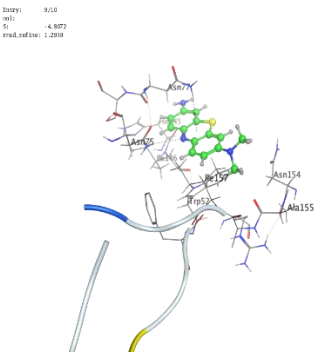

Fig. 23 3D of the binding mode of Giemsa Stain dye with (7N0R) receptor

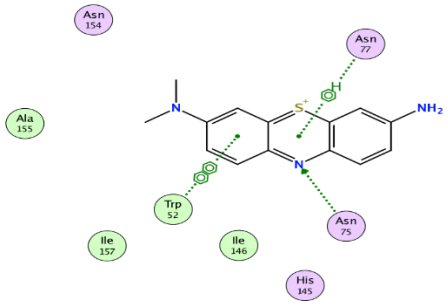

Fig. 24 2D of the binding mode of Giemsa Stain dye with (7N0R) receptor.

7N0R: VIRAL PROTEIN/IMMUNE SYSTEM / 7N0R

Ligand	Receptor				Interaction	Distance	E (kcal/mol)
O 4	NH1	ARG	107	(B)	H-acceptor	2.81	-8.8
O 4	NH2	ARG	107	(B)	H-acceptor	3.29	-0.6
O 5	N	ALA	156	(B)	H-acceptor	2.94	-3.4
O 6	OH	TYR	109	(B)	H-acceptor	2.84	-2.6
O 9	NH1	ARG	149	(B)	H-acceptor	2.93	-5.0
O 3	NH2	ARG	149	(B)	Ionic	3.01	-4.4
O 4	NH1	ARG	107	(B)	Ionic	2.81	-5.9
O 4	NH2	ARG	107	(B)	Ionic	3.29	-2.8
O 5	NH1	ARG	149	(B)	Ionic	3.60	-1.5
O 9	NH1	ARG	149	(B)	Ionic	2.93	-5.0
O 9	NH2	ARG	149	(B)	Ionic	3.95	-0.6
6-ring	CB	THR	54	(B)	pi-H	4.03	-0.6
6-ring	N	ALA	55	(B)	pi-H	4.08	-1.1

Fig. 25 The orange G dye interaction report data with (7N0R) receptor.

7N0R: VIRAL PROTEIN/IMMUNE SYSTEM / 7N0R

Ligand	Receptor				Interaction	Distance	E (kcal/mol)
N 3	ND2	ASN	75	(B)	H-acceptor	3.50	-0.5
6-ring	ND2	ASN	77	(B)	pi-H	4.23	-1.1
6-ring	6-ring	TRP	52	(B)	pi-pi	3.78	-0.0

Fig. 26 The Giemsa Stain dye interaction report data with (7N0R) receptor.

4. Conclusions

As seen in (Table 9, 10), the stability constants and Gibbs free energies of complexation are increased by the increase in Orange G and Giemsa Stain dyes. (Table 11, 12) show that the thermodynamic parameters given are increased by the decrease in scan rate supporting the diffusion mechanism reaction.

References

1. Ye T., He Y. and Bourguet E., Adsorption and electrochemical activity: anin-situ electrochemical scanning tunneling microscopy study of electrode reactions and potential-induced adsorption of porphyrins. Journal of Physical Chemistry, 110, 6141-6147(2006).
2. Bard A.J. and Faulkner L.R. "Electrochemical Methods Fundamentals and Applications," 2nd Edition, Wiley, Hoboken (2004).
3. Nicholson R.S. and Irving S., Theory of stationary electrode polarography: single scan and cyclic methods applied to reversible, irreversible, and kinetic systems. Analytical Chemistry, 36, 706-723(1964).
4. Ye T., He Y. and Bourguet E., Adsorption and electrochemical activity: anin-situ electrochemical scanning tunneling microscopy study of electrode reactions and potential-induced adsorption of porphyrins. Journal of Physical Chemistry, 110, 6141-6147(2006).
5. Bard A.J. and Faulkner L.R. "Electrochemical Methods Fundamentals and Applications," 2nd Edition, Wiley, Hoboken (2004)
6. Nicholson R.S. and Irving S., Theory of stationary electrode polarography: single scan and cyclic methods applied to reversible, irreversible, and kinetic systems. Analytical Chemistry, 36, 706-723(1964).
7. Kissinger P. and William R.H. "Laboratory Techniques in electrochemical chemistry," 2nd Edition, Revised and Expand. CRC, Boca Raton (1996).
8. Ojo S.I.F., Patricia P., Olufunmilayo O.J. Assessment of Potassium Chromate Inhibition and Adsorption on Type A513 Mild Steel in Simulated Contaminated Media, Energy Procedia 119: 883-890(2017).
9. Ayeni A., Alam S. and Kipouros G., Electrochemical Study of Redox Reaction of Various Gold III Chloride Concentrations in Acidic Solution. Journal of Materials Science and Chemical Engineering, 6, 80-89(2018).
10. SanthyW., SafriI., Diana R.E. and Yeni W.H., Carbon-Based Electrode Application for Determination and Differentiation of Chromium Ion Species Using Voltammetric Method.Voltammetry, Procedia Chemistry (2015).
11. Hanck K.W., Laitinen H.A., Electrochemical Reduction of Potassium Chromate in the Presence of Zinc(II) and Cobalt(II) in Molten Lithium Chloride-Potassium Chloride Eutectic. The Electrochemical Society, J. Electrochem. Soe. 118, 1123-1128 (1971).
12. Saifullahi S.I., Atika I.M., Halimah F.B., Zakariyya U.Z. Removal of Orange G Dye from Aqueous Solution by Adsorption: A Short Review, Journal of Environmental Treatment Techniques 9(1), 318-327(2021).
13. Guoqiang G., Juan L. Zhixi Z., Ziran Y., Conglu Z., Xiaohong H., A novel magnetic nanoscaled Fe3O4/CeO2 composite prepared by oxidation-precipitation process and its application for degradation of orange G in aqueous solution as Fenton-like heterogeneous catalyst. Chemosphere, 168, 254-263(2017).
14. John K., Eleana K., Kyriakos B., Christos K., Alexis L., Decolorization of Orange-G Aqueous Solutions over C60/MCM-41 Photocatalysts. Applied Sciences, 9(9), 1958- 1969(2019).
15. Benselka-Hadj N.A., Bentouami A., Derrichea Z., Bettahar N., C. de Ménorval L., Synthesis and characterization of Mg–Fe layer double hydroxides and its application on adsorption of Orange G from aqueous solution. Chemical Engineering Journal, 169, 231-238(2011).
16. Viorica D., Simona M., Cucu M., Romeo I.O., Rodica B., Mihai D., Ion B., A new heterogeneous

catalytic system for decolorization and mineralization of Orange G acid dye based on hydrogen peroxide and a macroporous chelating polymer.Dyes and Pigments, 95(1), 79-88(2012).
17. Yan W., Ricky P., Hui Z., Yao-Hui H., Degradation of the azo dye Orange G in a fluidized bed reactor using iron oxide as a heterogeneous photo-Fenton catalyst. The Royal Society of Chemistry, 5, 45276-45283(2015).
18. Jiwan S., Uma, Sushmita Banerjee., Yogesh C.S. A Very Fast Removal of Orange G from its Aqueous Solutions by Adsorption on Activated Saw Dust: Kinetic Modeling and Effect of Various Parameters. International Review of Chemical Engineering, 4(1), ISSN 2035-1755(2012).
19. Marwa S.S., Mohamed M.E., Esam A.G., Molecular Thermodynamics for the Redox Reaction of Sodium Tetrachloroaurate, $NaAuCl_4$ (Noble Material) with Giemsa Stain (GS) Dye in HNO_3 Solution Using Cyclic Voltammetry, Egyptian Journal of Chemistry. DOI: 10.21608/ejchem.2022.151756.6572.
20. Esam A.G., Moged A.B., Mohamed R.M., Fathy M.E., Hader M.F., Synthesis and Theoretical Calculating Properties of 2-(2-Cyanoacetamido)-4,5-Dimethylthiophene-3-Carboxamide (2-CDTC). Journal of Materials and Environmental Sciences, 10(2), 187-194(2019).
21. Lailla L.A., Shimaa A.A., Essam A.G., Sameh G.S., Theoretical Study of 1, 4-Dioxane in Aqueous Solution and Its Experimental Interaction with Nano-$CuSO_4$. Iranian Journal of Chemistry and Chemical Engineering, 38(3), 43-60(2019).
22. Essam A.G., Rania R. Z., Mai S. N., Cyclic Voltammetry Studies for the Interaction of CuCl2 with 4-Fluoro Benzoic Acid (FBA) in KBr Aqueous Solutions. Advanced Journal of Chemistry-Section A, 3(5), 583-593(2020).
23. Cotton F.A., Wilkinson G., John W., Sons, Advanced Inorganic Chemistry, 4th Edition, New York. (1980).
24. Prakash L.T., Gouri A.H., Sharanappa T.N.,Permanganate oxidation of chromium(III) in aqueous alkaline medium: a kinetic study by the stopped-flow technique. Transition Metal Chemistry, (22), 193–196(1997).
25. Abd El-Hady M.N, Gomaa E.A., .Zaky R.R. and Gomaa A.I., Synthesis, characterization simulation, cyclic voltammetry and biological studies on Cu(II), Hg(II) and Mn(II) complex of 3-(3,5-dimmethylpyrazol-1-yl)-3oxoproionnitrile. Journal of Molecular Liquids, 305,112794(2020).
26. Wang Y., Hernandes R.M, Bartlett D.J., Bingham J.M., Kline T.R., Sen A., and Mallouk T.E., Biopolar electrochemical mechanism for the propulsion of catalytic nanomotors in hydrogen peroxide solutions. Langmuir, 22(25), 10451-10456(2006).
27. El-Askalany A.M.E.H. and Abou El-Magd A.M., Stability constants of Zn(II),Pd(II),Cd(II) and Cu(II) complexes with hematoxylin. Chemical and Pharmaceutical Bulletin, 43(10), 1791-1792(1995).
28. Gomaa E.A., Abu-Qarn R.M., Ionic association and thermodynamic parameters for solvation of vanadyl sulfate in ethanol-water mixtures at different temperatures. Journal of molecular liquids, 232, 319-324(2017).
29. Gomaa E.A., Tahoon M.A., Ion association and solvation behavior of copper sulfate in binary aqueous-methanol mixtures at different temperatures. Journal of Molecular Liquids, 214, 19-23(2016).
30. Gomaa E.A., Zaky R.R. and Shokr A., Estimated the physical parameters of lanthanum chloride in water-N,N-dimethyl formamide mixtures using different techniques. Journal of Molecular liquids, 242, 913-918(2017).
31. Gomaa E.A., Zaky R.R. and Shokr A., Effect of calcon carboxylic acid on association process of vanadyl sulfate in water-N,N-dimeyhyl formamide mixed solvents. Chemical Data Collications, 11, 67-76(2017).
32. Esam A.G., Amr N., Mohamed A.T., Conductometric and volumetric study of copper sulphate in aqueous ethanol solutions at different temperatures. Journal of Taibah University for Science, 11(5), 741-748(2017).
33. El-Shereafy S.E., Esam A.G., Yousif A.M., El-Yazed A.S., Electrochemical and Thermodynamic Estimations of the Interaction Parameters for Bulk and Nano-Silver Nitrate (NSN) with Cefdinir Drug Using a Glassy Carbon Electrode. Iranian Journal of Materials Science & Engineering, 14(4), 48-57(2017).
34. Kim J.I., Cecal A., Born H.J. and Gomaa E.A., Preferential solvation of single ion: acritical study of the Ph4AsPh4B assumption for single ion thermodynamics in mixed aqueous acetonitrile and aqueous -N,N-dimethyl formamide solvents. Z. Phys. Chem., Neue Folge, 110, 209-216(1978).

35. Kim J.I. and Gomaa E.A., Preferential solvation of single ion: the Ph4AsPh4B assumption for single ion thermodynamics in mixed dimethylsulfoxide-water solvents. Bull. Soc. Chim. Belg, 90, 391(1981).
36. Ghandour M.A., Abo-Doma R.A. and Gomaa E.A. The Electroreduction (Polarogaphically) of uranyl ion in nitric acid methanol mixture media. Electrochim. Acta, 27, 159(1982).
37. Brownson D.A.C. and Banks C.E., "The Handbook of Graphene Electrochemistry," Springer (2014).
38. Gomaa E.A. and Tahoon M.A., Ion association and solvation behavior of copper sulfate in binary aqueous-methanol mixtures at different temperatures. Journal of Molecular Liquids, 214, 19-23(2016).
39. Wang J., Wiley J. and Sons, "Analytical Electrochemistry," 3rd ed., London (2006).
40. Gomaa E. A., Tahoon M. A., Shokr A., Ionic association and solvation study of CoSO4 in aqueous - organic solvents at different temperatures. Chemical Data Collections, 3–4, 58–67(2016).
41. Esam A.G., Mahmoud H.M., Mohamed G.M., Eman M.E., Cyclic voltammetry for the interaction between bismuth nitrate and methyl red in potassium nitrate solutions.Chemical Methodologies, 3(1), 1-11(2018).
42. Gomaa E.A., Begheit G.M., Polarographic and ConductometricStudies of Uranyl Ion in Sulphuric Acid-Ethanol Media. Asian Journal of Chemistry, 2: 444(1990).
43. Gomaa E.A., The polarographic electroreduction of uranyl ion in arsenic acid solution. J Monatshefte fur Chemie 119:287(1988).
44. Ghandour M.A., Gomaa E.A. and Abo Doma R.A., Polarographic behaviour of uranyl ion in maleate buffer solutions. Monatisheftr fur Chemie, 116, 33-42 (1985).
45. Abd El-Hady M.N., Gomaa E.A., Zaky R.R., Gomaa A.I., Synthesis, characterization, computational simulation, cyclic voltammetry and biological studies on Cu(II), Hg(II) and Mn(II) complexes of 3-(3,5-dimethylpyrazol-1-yl)-3-oxopropionitrile, 305, 112794(2020).
46. Esam A.G., Radwa T.R., Thermal and thermodynamic parameters for glycine (GL) solvation in water theoretically. Biomedical Journal of Scientific & Technical Research, 23(2), 17345-17348A(2019)
47. Kelly C.P., Cramer C.J. and Truhlar D.G., Aqueous solvation free energies of ions and ion−water clusters based on an accurate value for the absolute aqueous solvation free energy of the proton. J. Phys. Chem. B, 110, 32, 16066–16081(2006).
48. Winget P., Cramer C.J., and Truhlar D.G., Computation of equilibrium oxidation and reduction potentials for reversible and dissociative electron-transfer reactions in solution. Theoretical Chemistry Accounts, 112(4), 217-227(2004).
49. Zhu N., et al., A Novel Coronavirus from Patients with Pneumonia in China, 2019. N Engl J Med, 382, 727-733(2020).
50. Fehr, A.R., Perlman S., Coronaviruses: an overview of their replication and pathogenesis. Methods Mol Biol 1282, 1-23(2015).
51. Zhou, P. et al., A pneumonia outbreak associated with a new coronavirus of probable bat origin. Nature 579, 270-273(2020).